

## Fast and slow quenches in nucleation: Comparison of the theory with experiment and numerical simulations

I. Edrei and M. Gitterman

*Department of Physics, Bar-Ilan University, 52100 Ramat-Gan, Israel*

(Received 21 December 1984)

Numerical estimates of the time lag, the distribution function, and the flux of nuclei show that the differences between slow and fast quenches can be seen only if the critical nucleus has a comparatively large radius. In this case, a clear dependence on the quench rate appears, which hopefully might be observed in laboratory experiments and numerical simulations.

Recently, we formulated a new approach to time-dependent effects in nucleation theory.<sup>1,2</sup> One usually assumes that the stationary regime sets in immediately after a quench from a stable into a metastable state. The transition time  $\Theta$  ("the incubation time," "the time lag") has been considered by some authors (see review in Ref. 3) and found to be very small ( $10^{-5}$ – $10^{-6}$  sec), at least for liquid systems. We have shown, however,<sup>1,2</sup> that in some cases  $\Theta$  is not small, it may reach dozens of seconds. Moreover, it turned out that one has to distinguish between "slow" and "fast" quenches. It is in the latter case that  $\Theta$  increases drastically, and this leads to a much longer decay time of a metastable state. The distinction between the slow and fast quenches has the following simple physical meaning. The metastable state that appears after a quench is a state of incomplete equilibrium. In contrast to a slow quench, only small nuclei of a new phase are in equilibrium immediately after a fast quench. Therefore, it takes a long time for the nonstationary flux to set up a steady-state distribution of nuclei, and these transient processes cannot be neglected.

It is not surprising why previous investigators have overlooked this effect. They did not study the dependence of the time lag on the initial conditions, and assumed it was obvious that all transient processes are determined by the potential barrier for nucleation. Accordingly, all the integrals involved were calculated by the method of the steepest descents near the barrier.

Some experiments have been performed under different quench rates. Howland, Wong, and Knobler studied<sup>4</sup> the influence of the quench rate on the temperature distribution in the experimental cell. Different quench rates have been used by Ahlers, Cross, Hohenberg, and Safran<sup>5</sup> in a different dynamic problem in which a system passes through an instability point in the Rayleigh-Benard convection. We do not know, however, of any experimental study of the dependence of the time lag on the initial conditions.

Another powerful method of investigation of nucleation phenomena is by numerical simulation. There are indications of the importance of the rate of quench. Molecular dynamics studies under different quench factors (rescaling of the velocity of every particle at each time step) show a dependence of the onset of the nucleation process on the quench rate (see Fig. 2 in Ref. 6). Numerical solutions of the system of the time-dependent differential equation describing the nucleation (for different sizes of nuclei) indicate that the time lag depends on the minimal size of the nuclei present in equilibrium concentration (Fig. 1 in Ref. 3). There are, however, no systematic numerical studies

where nucleation processes have been studied under different quenching rates.

The relaxation of a metastable state is usually described<sup>7</sup> by the distribution function  $W(r,t)$  of nuclei of size  $r$  at time  $t$ . The variation of  $W(r,t)$  is determined by the change of the flux  $J(r,t)$  of nuclei according to the continuity equation

$$\frac{\partial W}{\partial t} = -\frac{\partial J}{\partial r}; \quad J = -FW - D\frac{\partial W}{\partial r} \quad (1)$$

To solve the Fokker-Planck equation (1) for  $W(r,t)$ , one has to know the explicit form of the functions  $F(r)$  and  $D(r)$  which determined the systematic growth (decay) and the diffusive growth of the nuclei, respectively. One usually assumes some model expressions for  $F(r)$  and  $D(r)$ . We have shown, however, that there is no need for additional assumptions; not too far from the critical point these two functions are fully determined by the critical dynamics,<sup>1</sup> namely, for the nonconserved order parameter.

$$F(r) = 2c\Gamma \left[ \frac{1}{r} - \frac{1}{r_c} \right]; \quad D(r) = c\Gamma \frac{D_0}{r^2}; \quad D_0 = \frac{kT}{4\pi\sigma} \quad (2)$$

where  $c\Gamma$  is the diffusion coefficient far from the critical points. The parameter  $D_0$  is determined by the surface tension  $\sigma$  and the temperature  $T$ . Since it has the dimension of length squared, it can be estimated as the square of a correlation length  $\xi$   $D_0 \sim \xi^2$ . Expressions similar to (2) have been obtained for the conserved order parameter.<sup>2</sup>

The important parameter of the nucleation theory is the so-called critical radius  $r_c$ , which determines the competition between the volume and surface parts of the nucleus energy. In fact, those nuclei with  $r < r_c$  will shrink and those with  $r > r_c$  will grow in time. All our consideration relates to the first stage of the decay of a metastable state before a substantial number of critical nuclei appear. The second part of the transition from a metastable to stable state has to be considered separately, using, for example, Eq. (1), but with the correlation radius changing in time.

We considered the vicinity of the critical point in order to find the form of the functions  $D(r)$  and  $F(r)$ . Our main results, however, have more extensive applications. For example, they do not depend on the divergence of the correlation length near the critical point. Notice, however, that, as was shown by Langer,<sup>8</sup> the statistical-mechanical approach to a metastable state may, strictly speaking, be handled only in the vicinity of the critical points. The reason is that the theoretical consideration of metastable states requires some additional constraints, say the coarse-graining procedure,

i.e., an introduction of a minimal length. The correlation length  $\xi$  is the natural minimal cutoff length near the critical points. Accordingly, we consider nuclei with radii  $r$ , satisfying the condition  $\xi < r < r_c$ . The critical radius  $r_c$  tends to infinity as one approaches the coexistence curve. Hence, by assuming  $\xi^2/r_c^2 < 1$ , we restrict ourselves to some region on the phase diagram which is located near the coexistence curve, but is not too close to the critical point.

We are interested in the time-dependent solution of Eq. (1). For this, we use the form

$$W(r, t) = W_{ss} + \sum_n A_n X_n(r) e^{-\lambda_n t}, \quad (3)$$

where  $W_{ss}(r)$  is the steady-state distribution function. The nonstationary flux  $J(r, t)$  is described by similar expansion.

The initial conditions are of fundamental importance in our considerations. Immediately following the quench, the system is in a state of incomplete equilibrium characterized by some characteristic length  $\lambda$  such that a steady-state distribution after a quench has been achieved only for nuclei

$$A_{n, \text{slow}} = \begin{cases} (-1)^{n/2+1} 2^{-1/2} (\pi D_0)^{-1/4} r_c W_{ss}^{1/2}(\xi) (1 - \lambda^2/r_c^2) (n!)^{-1/2} [(n-1)!!] \exp(-r_c^2/6D_0), & n = \text{even} \\ 0, & n = \text{odd} \end{cases} \quad (6)$$

By contrast, the results for fast quenches are significantly different from those for a slow one. The main contribution to the integral (5) comes now from nuclei of radii far from  $r_c$  and we found that<sup>1</sup>

$$A_{n, \text{fast}} = (-1)^{n+1} \Gamma\left(\frac{3}{4}\right) (2D_0)^{1/2-n/2} \pi^{-1/4} r_c^{n-1/2} W_{ss}^{1/2}(\xi) (n!)^{-1/2} \exp\left(\frac{-r_c^2}{8D_0}\right), \quad (7)$$

where  $\Gamma(X)$  is the gamma function.

The expressions for  $A_n$  [Eqs. (6) and (7)] for slow and fast quenches have been used in Refs. 1 and 2 for the calculation of the observable quantity  $N(t) = \int_0^t J(r_c, \tau) d\tau$ , the so-called integrated flux, i.e., number of critical nuclei appearing during the time  $t$ . Consideration of the integrated flux allows an answer to the following important question: What is the duration of the transient regime until the stationary state appears? A schematic plot of  $N(t)$  is shown in Fig. 1. Only after some characteristic time lag  $\Theta$  does the integrated flux start to be linear in time,  $N(t) = J_{ss}t$ . We bring here the final formulas for  $\Theta$  obtained in Ref. 1, for the slow and fast quenches.

$$\Theta_s = r_c^2/4c\Gamma, \quad (8)$$

$$\Theta_f = \Theta_s \nu; \quad \nu = 2\Gamma\left(\frac{3}{4}\right) \left(\frac{r_c^2}{4D_0}\right)^{-3/4} \exp\left(\frac{r_c^2}{24D_0}\right). \quad (9)$$

As is to be expected,  $\nu \gg 1$ , and the time lag exponentially increases for the fast quenches.

However, for a comparison with experiments, one has to calculate the distribution function  $W(r, t)$  and the flux  $J(r, t)$  during the transient period. With expressions (6) and (7) for  $A_n$  and  $\lambda_n$ , one can find<sup>1</sup> both the transient distribution function  $W(r, t)$ , given by Eq. (3) and the flux  $J(r, t)$ . The general line of calculations is the same as in Refs. 1 and 2. We bring here only final results, subject to the following important comment. In Eq. (3) one has to perform summation over  $n$ , which turns out to be different for slow and fast quenches. For the case of the slow

of size  $r < \lambda$ . Therefore, the initial conditions are

$$W(r, 0) = W_{ss}(r) \Theta(\lambda - r), \quad (4)$$

where  $\Theta(\lambda - r)$  is the unit step function. For "slow" quenches  $\lambda \rightarrow r_c$  and for "fast" quenches  $\lambda \rightarrow \xi$ .

The coefficients  $A_n$  in Eq. (3) are determined by the initial conditions. One readily finds that

$$A_n = - \int_{\lambda}^{r_c} X_n(r) dr. \quad (5)$$

It turns out that the integrand in (5) is a monotonically decreasing function of  $r$ . Thus, the main contribution to the integrand comes from its lower limit, i.e.,  $\lambda$ , which according to Eq. (4) depends on the speed of the quench. Only in the case of a slow quench does the main contribution to (5) come from the vicinity of  $r_c$  so that one can use the method of steepest descents, just as is usually done for the steady-state case.

For slow quenches, an integral obtained by substituting a solution of Eqs. (1) and (2) has been calculated by the method of steepest descent in Ref. 1. The final result is

quench, the series in  $n$  are very slowly convergent, and one has to take into account the terms with large  $n$ . It is hard, however, to find these terms by simple methods.<sup>1,2</sup> The terms of higher order in  $n$  are important for the small times  $t$ . Therefore, one has to perform a cutoff at small  $t$  in  $W(r, t)$  and  $J(r, t)$  for the case of slow quench. On the other hand, for fast quenches all calculations are much more precise, and one needs no cutoff for this case.

We bring here the results of calculations for the nonconserved order parameter. The time dependence of the nucleation in systems with conserved order parameter looks

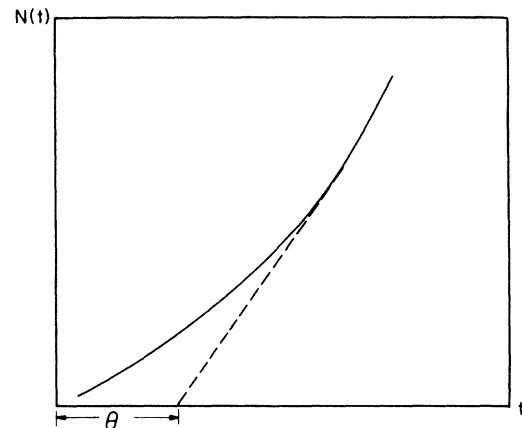


FIG. 1. Time dependence of the integrated flux  $N(r, t)$ .

similar.

$$W_{\text{slow}}(r,t) = W_{\text{ss}} - 2f(r_c)[rW_{\text{ss}}(r)]^{1/2} \frac{\exp(-2c\Gamma t/r_c^2)}{(2c\Gamma t/r_c^2)^{1/2}}, \quad (10)$$

$$J_{\text{slow}}(r,t) = J_{\text{ss}} + f(r_c)c\Gamma D_0 2^{1/2}[r^{-5}W_{\text{ss}}(r)]^{1/2}g(r) \frac{\exp(-2c\Gamma t/r_c^2)}{(2c\Gamma t/r_c^2)^{1/2}}, \quad (11)$$

where

$$f(r_c) = \left(\frac{r_c}{\pi D_0}\right)^{1/2} \frac{1 - \lambda^2/r_c^2}{4} W_{\text{ss}}^{1/2}(\xi) \exp\left[-\frac{r_c^2}{6D_0}\right], \quad g(r) = \frac{1}{2} + \frac{r^2}{D_0} - \frac{r^3}{D_0 r_c} - \frac{r^2}{\sqrt{2}D_0} + \frac{r^4}{\sqrt{2}D_0 r_c^2}. \quad (12)$$

As was mentioned above, one has to make the cutoff of small  $t$  in Eqs. (10) and (11), which behave nonphysically in this region.

$$W_{\text{fast}}(r,t) = W_{\text{ss}} - \left(\frac{4D_0}{\pi^2}\right)^{1/4} \frac{\Gamma(3/4)}{r_c} W_{\text{ss}}^{1/2}(\xi) e^{-r_c^2/8D_0} [W_{\text{ss}}(r)r]^{1/2} \exp\left[-\left(\frac{r^2 - r_c^2}{2r_c\sqrt{2}D_0}\right)^2\right] \\ \times \exp\left[-\frac{2c\Gamma}{r_c^2}t\right] \exp\left[\frac{r_c^2 - r^2}{2D_0}\right] \exp\left[-\frac{2c\Gamma}{r_c^2}t\right] - \frac{r_c^2}{4D_0} \exp\left[-\frac{4c\Gamma}{r_c^2}t\right], \quad (13)$$

$$J_{\text{fast}}(r,t) = J_{\text{ss}} + \frac{(2D_0^{5/2})^{1/2}c\Gamma\Gamma(3/4)W_{\text{ss}}^{1/2}(\xi)}{\pi^{1/2}r_c} e^{-r_c^2/8D_0} [W_{\text{ss}}(r)r^{-5}]^{1/2} \exp\left[-\left(\frac{r^2 - r_c^2}{2r_c\sqrt{2}D_0}\right)^2\right] \\ \times \exp\left[-\frac{2c\Gamma}{r_c^2}t\right] \exp\left[\frac{r_c^2 - r^2}{2D_0}\right] \exp\left[-\frac{2c\Gamma}{r_c^2}t\right] - \frac{r_c^2}{4D_0} \exp\left[-\frac{4c\Gamma}{r_c^2}t\right] \left[ g(r) - \frac{r^2}{D_0} \exp\left[-\frac{2c\Gamma}{r_c^2}t\right] \right], \quad (14)$$

with  $g(r)$  defined in Eq. (12).

Note that for both slow and fast quenches  $W(r,t)$  and  $J(r,t)$  show the same time dependence. In addition, the general form of the  $r$  dependence for  $W_{\text{slow}}$  and  $W_{\text{fast}}$  is very similar.

For comparison of the theoretical results (10)–(14) with experiment and numerical simulations, it is convenient to present these results graphically. For all numerical estimates we use the typical value of the diffusion coefficient  $c\Gamma$  of liquids far away from the critical point,  $c\Gamma = 10^{-5}$  cm<sup>2</sup>/sec. Two additional parameters, the radius of the critical nucleus  $r_c$ , and  $D_0$  which is of the order of the square of the correlation length,  $\xi^2$ , are crucially dependent on the thermodynamical state of a metastable system immediately after a quench. Although all of our approach is correct only if the condition  $r_c > \xi$  is fulfilled, the magnitudes of  $r_c$  and  $\xi$  might be changed within reasonable limits. One can assume, for example,  $10^{-8}$  cm  $< \xi < 10^{-6}$  cm;  $10^{-7}$  cm  $< r_c < 10^{-4}$  cm, provided that  $r_c > \xi$ .

The time lag  $\Theta$  as a function of a radius of the critical nucleus  $r_c$  [Eqs. (8) and (9)] is shown in Fig. 2. In the construction of Fig. 2 it is assumed that  $\xi$  is equal to  $4.10^{-7}$  cm. From Fig. 2 it transpires that an appreciable difference in the time lags for slow and fast quenches occurs only for  $r_c \geq 4.10^{-6}$  cm (or from  $r_c \approx 10^{-6}$  cm for  $\xi = 10^{-7}$  cm). Therefore, for small  $r_c$ , as is commonly used in the computer simulations, the difference between slow and fast quenches cannot be observed, at least from the time lag measurements.

Immediately following a quench, the distribution function of nuclei  $W(r,0)$  is described by Eq. (4), which is quite different for slow ( $\lambda \rightarrow r_c$ ) and fast ( $\lambda \rightarrow \xi$ ) quenches. On the other hand, after a time of the order of  $\Theta$ , the distribution functions in both cases approach the steady-state value for all nucleus radii smaller than the critical one.

In Fig. 3 we depict the distribution function  $W$  vs  $t$  for

some typical radius of nucleus  $r = 5.10^{-7}$  cm ( $r_c = 8.10^{-6}$  cm,  $\xi = 4.10^{-7}$  cm). This typical form of the graph is the same for all radii of nuclei and bears a resemblance to those obtained in numerical simulation.<sup>3</sup>

As distinct from the distribution function, the time dependence of the flux of nuclei  $J(r,t)$  is significantly different for small and large values of the radius of the critical nucleus  $r_c$ , especially for fast quenches. For small  $r_c$ ,  $J(r,t)$  manifests maxima before the transient fluxes reach the steady-state values ("over shooting") which have been seen in computer simulations.<sup>3</sup> However, in addition to such maxima, our calculations show up a minima of  $J(r,t)$  for large  $r_c$ . All this nonmonotonic behavior takes place solely for fast quenches, while for slow quenches  $J(r,t)$  (for not too small times) is a monotonic function of time.

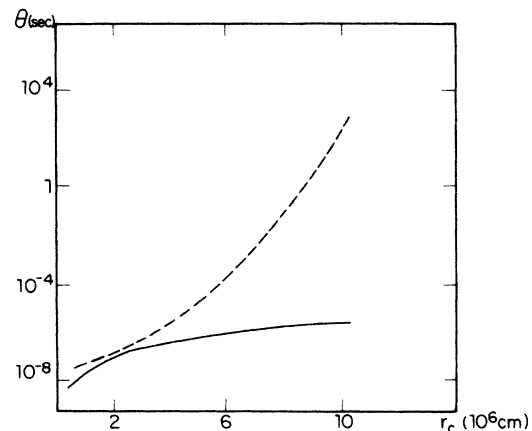


FIG. 2. Time lag  $\Theta$  as a function of radius of the critical nucleus  $r_c$  (the solid line, slow quenches; the dotted line, fast quenches).

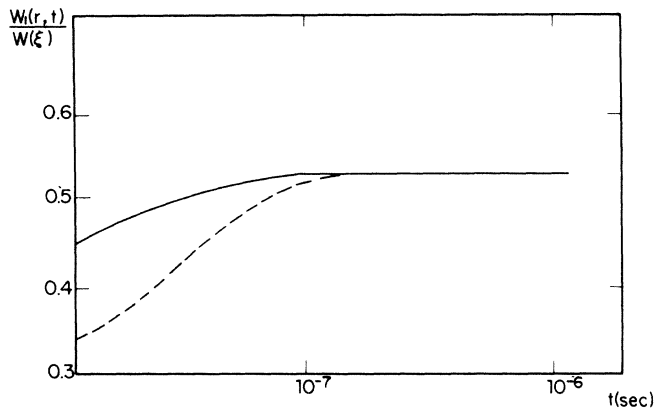


FIG. 3. Distribution function vs time for some typical radius of nucleus,  $r = 5 \times 10^{-7}$  cm (—, slow quench; · · · ·, fast quench).

To the best of our knowledge, there are no experiments or numerical simulations concerning nucleation for different rates of quench. In numerical calculations one usually assumes that only nuclei of a minimal size are in equilibrium immediately after a quench (and, in fact, during all the nucleation process). This means, in our language, that  $\lambda = \xi$  in Eq. (4), i.e., all numerical simulations are performed for the fast quench. Unfortunately, the number of particles used at present in numerical simulations is comparatively small, so that  $r_c$  is of order of  $10^{-7}$  cm.<sup>3</sup> According to Fig. 2, we predict that the time lag will drastically increase with increasing radius of the critical nucleus. Another new feature, which will become apparent at larger  $r_c$ , is a transition from maxima to minima in time dependence of the transient flux of nuclei  $J(r, t)$ . It would be of interest, therefore, to increase as much as possible,  $r_c$  in the numerical simulation or maybe to perform them in two dimensions.

We have recently<sup>9</sup> performed the Monte Carlo simulations for the three-dimensional  $168 \times 168 \times 168$  Ising lattice in the framework of the Glauber dynamics. For the different fast quenches, in agreement with the theoretical prediction (9), the time lag is found to be exponentially, rather than linearly, dependent on the squared radius of the critical nucleus.

A real experiment is quite the opposite to numerical

simulations with respect to the size of  $r_c$ . It is very hard to observe very small nuclei, not to mention the speedy completion of the decay of a metastable state for small  $r_c$ . While larger values of  $r_c/\xi$  increase the differences between slow and fast quenches, they also lead to a drastic (exponential) decrease of the steady-state nucleation rate,  $J_{ss}$ . The rather small value of  $J_{ss}$  for such quenches indicates that the lifetime of a metastable state is large. We are interested, however, in the length of the time interval between the end of the quench and the beginning of the steady state regime, rather than a complete decay of the metastable state. The beginning of the steady state is determined experimentally by the linear increase of  $N(r_c, t)$  with time. In order to check this linear dependence, it is enough, in fact, to see only a few droplets larger than  $r_c$ . Then one has to perform a "fast" quench, finding thereby the time lag  $\Theta_f$ . The next step is to measure the time lags  $\Theta_s$  for different "slow" quenches. The duration of such quenches is limited, of course, from above by  $\Theta_f$ . In principle, one can measure the transient distribution function  $W(r, t)$  as well.

Numerical estimates of both  $\Theta_f$  and  $J_{ss}$  are extremely sensitive to the values of  $r_c$  and  $\xi$ , i.e., to the distance of the quenched state both from the coexistence curve and from the critical point. Note, however, that experimentalists can perform a quench into a state with known  $r_c/\xi$  (equal to 7, 10, and 20 in Ref. 10) and reasonable value of  $J_{ss}$ . Our estimates can provide only a general guide for experimental setups. For example, for  $r_c/\xi = 15$ , the difference between fast and slow quenches is considerable ( $\Theta_f/\Theta_s \approx 130$ ) while  $\ln J$  equals zero (i.e., one nucleus per second is produced in  $1 \text{ cm}^3$ ) for  $r_c \approx 4.5 \cdot 10^{-6}$  cm, and is  $-20$  for  $r_c = 2 \cdot 10^{-4}$  cm. If  $r_c/\xi = 12$ , then  $\Theta_f/\Theta_s = 15$  and  $J = 1 \text{ (cm}^3 \text{ sec)}^{-1}$  for  $r_c = 2 \cdot 10^{-4}$  cm.

Both regimes of slow and fast quenches can be realized experimentally. Very fast quenches, of order of a few msec, can be obtained by pressure jumps,<sup>11</sup> along with slow quenches achieved by temperature changes.

In addition to liquids considered above, the transient processes in nucleation are even more profound for the solid systems.

We are looking for experimental manifestations of the influence of different quench rates on the nucleation processes, both in numerical simulations and in laboratory experiments.

<sup>1</sup>Y. Rabin and M. Gitterman, Phys. Rev. A **29**, 1496 (1984).

<sup>2</sup>M. Gitterman, I. Edrei, and Y. Rabin, in *Application of Field Theory to Statistical Mechanics*, edited by L. Garrido, Lecture Notes in Physics, Vol. 216 (Springer, Heidelberg, 1984).

<sup>3</sup>K. F. Kelton, A. L. Greer, and C. V. Thompson, J. Chem. Phys. **79**, 6261 (1983).

<sup>4</sup>R. G. Howland, N. C. Wong, and C. M. Knobler, J. Chem. Phys. **73**, 522 (1980).

<sup>5</sup>G. Ahlers, M. C. Cross, P. C. Hohenberg, and S. Safran, J. Fluid Mech. **110**, 297 (1981).

<sup>6</sup>R. Mountain and P. K. Basu, J. Chem. Phys. **78**, 7318 (1983).

<sup>7</sup>*Nucleation*, edited by A. C. Zettlemoyer (Dekker, New York, 1969).

<sup>8</sup>J. S. Langer, Ann. Phys. (N.Y.) **41**, 108 (1967); **54**, 258 (1969); **65**, 53 (1971).

<sup>9</sup>I. Edrei and M. Gitterman, J. Phys. A. (to be published).

<sup>10</sup>S. Krishnamurty and W. I. Goldberg, Phys. Rev. A **22**, 2147 (1980).

<sup>11</sup>N. C. Wong and C. M. Knobler, J. Chem. Phys. **66**, 4707 (1977).